

# Ultraflexible amorphous silicon transistors made with a resilient insulator

Cite as: Appl. Phys. Lett. **96**, 042111 (2010); <https://doi.org/10.1063/1.3298364>

Submitted: 26 November 2009 . Accepted: 29 December 2009 . Published Online: 29 January 2010

Lin Han, Katherine Song, Prashant Mandlik, and Sigurd Wagner



View Online



Export Citation

## ARTICLES YOU MAY BE INTERESTED IN

**Electrical response of amorphous silicon thin-film transistors under mechanical strain**

Journal of Applied Physics **92**, 6224 (2002); <https://doi.org/10.1063/1.1513187>

**Failure resistance of amorphous silicon transistors under extreme in-plane strain**

Applied Physics Letters **75**, 3011 (1999); <https://doi.org/10.1063/1.125174>

**Mechanics of rollable and foldable film-on-foil electronics**

Applied Physics Letters **74**, 1177 (1999); <https://doi.org/10.1063/1.123478>

**HIDEN**  
ANALYTICAL

## Instruments for Advanced Science

Contact Hiden Analytical for further details:

W [www.HidenAnalytical.com](http://www.HidenAnalytical.com)  
E [info@hiden.co.uk](mailto:info@hiden.co.uk)

CLICK TO VIEW our product catalogue

### Gas Analysis

- dynamic measurement of reaction gas streams
- catalysis and thermal analysis
- molecular beam studies
- dissolved species probes
- fermentation, environmental and ecological studies

### Surface Science

- UHV TPD
- SIMS
- end point detection in ion beam etch
- elemental imaging - surface mapping

### Plasma Diagnostics

- plasma source characterization
- etch and deposition process reaction kinetic studies
- analysis of neutral and radical species

### Vacuum Analysis

- partial pressure measurement and control of process gases
- reactive sputter process control
- vacuum diagnostics
- vacuum coating process monitoring

# Ultraflexible amorphous silicon transistors made with a resilient insulator

Lin Han,<sup>a)</sup> Katherine Song, Prashant Mandlik,<sup>b)</sup> and Sigurd Wagner

Department of Electrical Engineering and Princeton Institute for the Science and Technology of Materials, Princeton University, Princeton, New Jersey 08544, USA

(Received 26 November 2009; accepted 29 December 2009; published online 29 January 2010)

The conventional, brittle, silicon nitride barrier layer and gate insulator in amorphous silicon thin-film transistors (a-Si:H TFTs) on 50  $\mu\text{m}$  thick polyimide foil was replaced by a resilient, homogeneous, hybrid of silicon dioxide and silicone polymer. The transistor structures can be bent down to 0.5 mm radius (5% strain) in tension and down to 1 mm radius (2.5% strain) in compression. This pronounced flexibility shifts the criterion for reversible bending away from a-Si:H TFT backplanes and toward the materials for substrate and encapsulation. It qualifies a-Si:H TFTs for pull-out display screens in handheld devices. © 2010 American Institute of Physics. [doi:10.1063/1.3298364]

Amorphous silicon is the most prominent candidate semiconductor for the thin-film transistor (TFT) backplane of flexible displays, by virtue of its advanced state of development and industrial dominance. Here we report how we made a-Si:H TFTs so bendable that they no longer limit deformation; their plastic substrate does. Bendability under uniaxial strain of up to 5% is achieved by employing a resilient insulator in place of brittle silicon nitride,  $\text{SiN}_x$ . The insulator is a homogeneous hybrid of  $\text{SiO}_2$  and silicone polymer that we introduced as a permeation barrier for organic light-emitting diodes (OLEDs)<sup>1</sup> and as a gate dielectric for a-Si:H TFTs.<sup>2</sup> Under nanoindentation this “hybrid” deforms viscoelastically<sup>3</sup> in contrast to  $\text{SiO}_2$  or  $\text{SiN}_x$ , which fracture. The hybrid forms excellent chemical<sup>1</sup> and electrical barriers<sup>2</sup> because it has properties close to those of  $\text{SiO}_2$  yet some polymeric character. The latter appears to prevent formation of the top-to-bottom microcracks that are responsible for chemical leaks in permeation barriers,<sup>4</sup> and for electrical leaks in thin gate insulators of plasma-deposited  $\text{SiN}_x$ . We now exploited the hybrid’s resilience for raising the bendability of a-Si:H TFTs on polymer foil substrates.

a-Si:H TFTs in the conventional inverted staggered, back-channel cut, geometry were made with a range of channel widths  $W$  and lengths  $L$  on passivated 50  $\mu\text{m}$  thick Kapton E polyimide foil. All layers that contain silicon were made by plasma-enhanced chemical vapor deposition. The schematic cross section of a hybrid TFT is shown in Fig. 1(a), and for comparison in Fig. 1(b) our standard 150 °C-process  $\text{SiN}_x$  TFT. Fabrication of the hybrid TFTs was kept as similar as was possible with our equipment to that for the conventional  $\text{SiN}_x$  TFTs.<sup>5</sup> The most important, but not directly relevant, difference is the air exposure of the hybrid gate dielectric during transfer to  $i$  a-Si:H channel layer deposition. The 10 nm of  $\text{SiN}_x$  interlayer for substrate passivation in the hybrid TFT serves as adhesive. In Figs. 1(a) and 1(b) note the following changes from  $\text{SiN}_x$  to hybrid that we made to enhance flexibility. (i) Substrate passivation and gate dielectric of hybrid instead of  $\text{SiN}_x$ . (ii) Thinner hybrid than the corresponding  $\text{SiN}_x$ . (iii) Composite and

thinner Cr/Al/Cr gate electrode and source/drain contacts replaced pure Cr.

Flexibility was tested by bending a given TFT around cylinders of successively smaller radii  $R$  around the axis shown in Fig. 1(c). The test sequence was as follows: electrical measurement/bending for 1 minute/flattening/electrical measurement. We monitored the changes in electrical characteristics, which turned out to be small, and electrical failure, which we translated to having surpassed a critical strain  $\epsilon_{\text{critical}}$ . We measured a TFT’s drain current  $I_{\text{DS}}$ —gate voltage  $V_{\text{GS}}$  transfer characteristic and gate-source leakage current

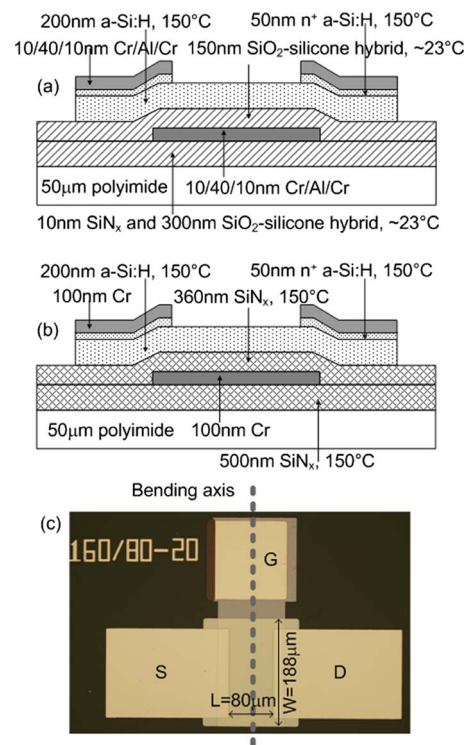


FIG. 1. (Color online) (a). Schematic cross section of highly bendable a-Si:H thin-film transistor made with hybrid substrate passivation and gate insulator; inscriptions show layer thickness, material, and process temperature. (b) Cross section of conventional flexible a-Si:H TFT made with  $\text{SiN}_x$  substrate passivation and gate insulator, shown for comparison. (c) Micrograph of completed hybrid TFT, showing the channel dimensions used in TFT evaluation, and the axis of bending.

<sup>a)</sup>Electronic mail: linhan@princeton.edu.

<sup>b)</sup>Present address: Universal Display Corporation, Ewing, New Jersey.

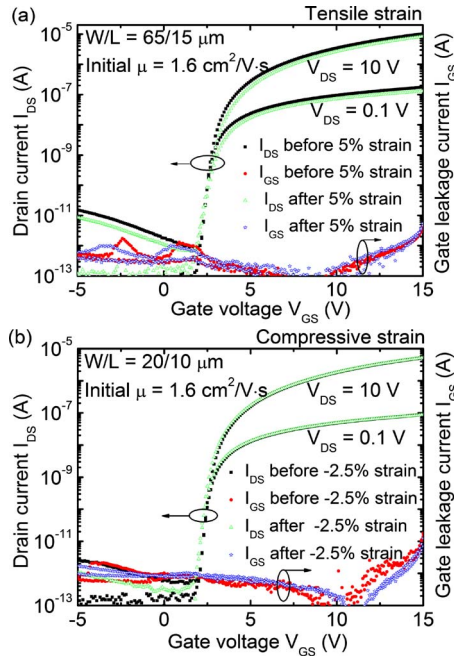


FIG. 2. (Color online) Transfer characteristics of two hybrid TFTs. (a) TFT bent to tensile strain. (b) TFT bent to compressive strain. TFTs were evaluated while reflattened after each bending step.

$I_{\text{leak}}$  (Fig. 2). From these we evaluated threshold voltage  $V_T$  and electron mobility  $\mu$  in the linear regime, ON current  $I_{\text{on}}$  at gate voltage  $V_{\text{GS}} = 15$  V, OFF current  $I_{\text{off}}$  at  $V_{\text{GS}} = -5$  V, and gate leakage  $I_{\text{leak}}$  current at  $V_{\text{GS}} = -5$  V (Fig. 3). The channel length  $L$  is the distance between the source and drain, and the channel width  $W$  is the width of the a-Si:H island, as shown in Fig. 1(c); the photomask dimensions are only their nominal values. Theory<sup>6</sup> and experience confirm that  $\varepsilon$  is approximated well by treating the TFT-on-substrate composite as a homogeneous sheet of thickness  $h$ , such that in bending to a cylinder  $\varepsilon = h/2R$ . This relation captures the two approaches to raising flexibility as follows: reducing  $h$ , a design parameter, and raising  $\varepsilon_{\text{critical}}$ , a materials property. Other important parameters that affect flexibility are device layer thickness  $d$ , which enters via  $\varepsilon_{\text{critical}} \propto 1/\sqrt{d}$ ,<sup>7</sup> and layer adhesion, which affects  $\varepsilon_{\text{critical}}$  in compression.

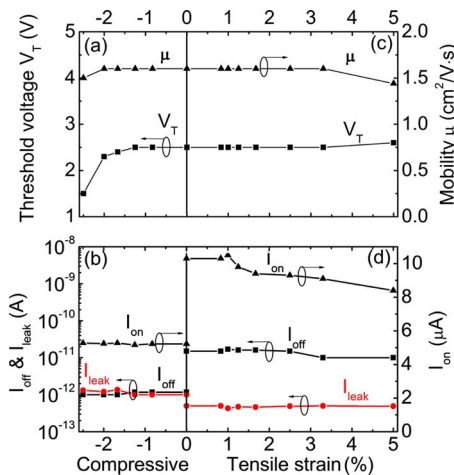


FIG. 3. (Color online) Performance parameters of the TFTs of Fig. 2, evaluated after each bending step and plotted against (a),(b) compressive, and (c),(d) tensile strain. (a),(b):  $W/L = 20/10$   $\mu\text{m}$ ; (c),(d):  $W/L = 65/15$   $\mu\text{m}$ .

Representative transfer characteristics of hybrid TFTs are shown before and after bending to the maximum tensile strain of +5% [Fig. 2(a)] and maximum compressive strain of -2.5% [Fig. 2(b)]. These transistors remained functional. Fig. 3 shows strain-point by strain-point data for the TFTs of Fig. 2; the points correspond to  $R = 3, 2.5, 2, 1.5, 1, 0.75$ , and 0.5 mm. 20 hybrid TFTs each were tested in tension and in compression. In tension, three TFTs failed during manipulation, 17 withstood bending to  $R = 0.75$  mm ( $\varepsilon = 3.3\%$ ), and two bending to  $R = 0.5$  mm ( $\varepsilon = 5\%$ ). In compression, 17 of 20 TFTs withstood bending to  $R = 1.25$  mm ( $\varepsilon = 2\%$ ), and five of 20 bending to  $R = 1.0$  mm ( $\varepsilon = 2.5\%$ ). During outward (tensile) bending cracks appeared first in the source/drain and gate contact pads and eventually in the channel, where cracks developed preferentially at the edge of the source/drain metal. During inward (compressive) bending, the TFTs peeled off first at the source/drain and in the channel.

The maximum tensile  $\varepsilon_{\text{critical}}$  of the hybrid TFTs of 5% is a factor of  $\sim 10$  higher than that of  $\text{SiN}_x$  TFTs, 0.5%.<sup>8</sup> The maximum compressive  $\varepsilon_{\text{critical}}$ , 2.5%, lies a bit higher than the already high value observed in  $\text{SiN}_x$  TFTs, 2%. The difference between tensile and compressive  $\varepsilon_{\text{critical}}$  arises from the different mechanisms that cause failure in tension and compression. In tension a device layer develops channel cracks, while in compression it breaks after the buckling that is coupled with delamination.<sup>8</sup> It is worth noting that the tensile  $\varepsilon_{\text{critical}}$  of  $\sim 1$   $\mu\text{m}$  thick a-Si:H was reported to be  $\sim 2\%$ .<sup>9</sup>

We take the very high values of  $\varepsilon_{\text{critical}}$  obtained to signal a qualitative shift in the conceptual approach to making TFT backplanes flexible, away from a focus on the TFTs toward one on the display devices, substrate and encapsulation. When placed in the neutral plane<sup>6,10</sup> the a-Si:H TFTs' integrity no longer is threatened by excessive bending. Instead, substrate foils and encapsulation layers are becoming the critical portions of the structures; they may break, become permeable, or deform permanently. For example, we observe a crease<sup>11</sup> in the 50  $\mu\text{m}$  polyimide foil substrate after it has been bent outward for 1 minute around  $R = 0.5$  mm, an extreme condition under which the corresponding TFTs of Figs. 2 and 3 remained intact.

Making wide-format pull-out displays for handheld devices will become possible if all components can be made as resilient as these hybrid a-Si:H TFTs. Typical handheld devices are  $\sim 7$  mm thick, thus can accommodate a spindle with a diameter of 3 mm that can grow to 5 mm when the roll-out display is retracted. Given a thickness of 100  $\mu\text{m}$ , an approximately 240 mm long, rollable, active-matrix OLED display will fit on the spindle. When combined with the typical handheld device length (=display height) of 100 mm, even the widescreen video aspect ratio of 2.35:1 can be accommodated.

A sizeable body of literature has been built over the past ten years on materials substitution for enhancing the flexibility of devices that incorporate brittle materials, or for retaining some flexibility in an inorganic-for-organic substitution. a-Si:H TFTs have been made with a two-layer gate dielectric of organic material/ $\text{SiN}_x$ .<sup>12</sup> Similar composites have been employed to improve the electric quality of the organic gate insulator in organic TFTs,<sup>13</sup> and to make the indium tin oxide (ITO) anode of OLEDs less brittle.<sup>14</sup> Complete substitution of a brittle material by an organic material has been reported

for the replacement of the ITO anode of OLEDs by an organic conductor<sup>15,16</sup> and for the fabrication of all-organic TFTs.<sup>17,18</sup> All-organic devices have been flexed<sup>19</sup> or deformed plastically<sup>16</sup> to strains of up to  $\sim 2.5\%$ . An important distinction of our results from earlier work is that we obtained the very high flexibility in high-performance a-Si:H TFTs, with a process quite similar to the one that is used widely in industry, and with devices that have excellent prospects for reaching the performance needed for powering flexible OLED pixel circuits.<sup>2,20</sup>

We thank Universal Display Corporation for supporting this research. L.H. gratefully acknowledges a Fellowship from the Princeton Program in Plasma Science and Technology.

- <sup>1</sup>P. Mandlik, J. Gartside, L. Han, I.-C. Cheng, S. Wagner, J. Silvernail, R. Ma, M. Hack, and J. J. Brown, *Appl. Phys. Lett.* **92**, 103309 (2008).
- <sup>2</sup>L. Han, P. Mandlik, K. H. Cherenack, and S. Wagner, *Appl. Phys. Lett.* **94**, 162105 (2009).
- <sup>3</sup>L. Han, P. Mandlik, J. Gartside, S. Wagner, J. Silvernail, R. Ma, M. Hack, and J. J. Brown, *J. Electrochem. Soc.* **156**, H106 (2009).
- <sup>4</sup>Y. Leterrier, *Prog. Mater. Sci.* **48**, 1 (2003).
- <sup>5</sup>H. Gleskova, S. Wagner, V. Gašparík, and P. Kováč, *J. Electrochem. Soc.* **148**, G370 (2001).

- <sup>6</sup>Z. Suo, E. Y. Ma, H. Gleskova, and S. Wagner, *Appl. Phys. Lett.* **74**, 1177 (1999).
- <sup>7</sup>Z. Suo, J. Vlassak, and S. Wagner, *China Particuology* **3**, 321 (2005).
- <sup>8</sup>H. Gleskova, S. Wagner, and Z. Suo, *Appl. Phys. Lett.* **75**, 3011 (1999).
- <sup>9</sup>S. Guha, W. den Boer, S. C. Agarwal, and M. Hack, *Appl. Phys. Lett.* **47**, 947 (1985).
- <sup>10</sup>T. Sekitani, S. Iba, Y. Kato, Y. Noguchi, T. Someya, and T. Sakurai, *Appl. Phys. Lett.* **87**, 173502 (2005).
- <sup>11</sup>G. Gu, P. E. Burrows, S. Venkatesh, S. R. Forrest, and M. E. Thompson, *Opt. Lett.* **22**, 172 (1997).
- <sup>12</sup>S. H. Won, J. K. Chung, C. B. Lee, H. C. Nam, J. H. Hur, and J. Jang, *J. Electrochem. Soc.* **151**, G167 (2004).
- <sup>13</sup>Q. Cao, M.-G. Xia, M. Shim, and J. A. Rogers, *Adv. Funct. Mater.* **16**, 2355 (2006).
- <sup>14</sup>S.-W. Cho, J.-A. Jeong, J.-H. Bae, J.-M. Moon, K.-H. Choi, S. W. Jeong, N.-J. Park, J.-J. Kim, S. H. Lee, J.-W. Kang, M.-S. Yi, and H.-K. Kim, *Thin Solid Films* **516**, 7881 (2008).
- <sup>15</sup>R. Paetzold, K. Heuser, D. Henseler, S. Roeger, G. Wittmann, and A. Winnacker, *Appl. Phys. Lett.* **82**, 3342 (2003).
- <sup>16</sup>R. Bhattacharya, S. Wagner, Y. J. Tung, J. Esler, and M. Hack, *Appl. Phys. Lett.* **88**, 033507 (2006).
- <sup>17</sup>T. Sekitani, S. Iba, Y. Kato, and T. Someya, *Jpn. J. Appl. Phys., Part 1* **44**, 2841 (2005).
- <sup>18</sup>M. S. Lee, H. S. Kang, H. S. Kang, J. Joob, A. J. Epstein, and J. Y. Lee, *Thin Solid Films* **477**, 169 (2005).
- <sup>19</sup>A. Jedaa and M. Halika, *Appl. Phys. Lett.* **95**, 103309 (2009).
- <sup>20</sup>B. Hekmatshoar, S. Wagner, and J. C. Sturm, *Appl. Phys. Lett.* **95**, 143504 (2009).